

# Comparative Studies of Magnetic Field Effect on Radical Pairs Photogenerated by Electron Transfer from Biphenyl to Derivatives of Phenyl Pyrilium Salt and to Corresponding Thio Salts

Partha Pratim Parui,<sup>†</sup> N. Monoj,<sup>‡</sup> D. N. Nath,<sup>†</sup> and Mihir Chowdhury<sup>\*,†</sup>

Department of Physical Chemistry, Indian Association for the Cultivation of Science, Jadavpur, Kolkata 700 032, India, and Photochemical Research Unit, Regional Research Laboratory, Trivandrum 695 019, India

Received: April 17, 2003; In Final Form: October 21, 2003

We have generated radical pairs (RPs) in SDS micellar medium by electron transfer from the ground state of biphenyl (BP) to various alkyl-substituted phenyl pyrilium cations (PP<sup>+</sup>) and corresponding thio-phenyl pyrilium cations (SPP<sup>+</sup>) and have compared the dynamics of RP recombination in magnetic fields varying from 0 to 5 T. A comparison of PP<sup>+</sup>/BP<sup>+</sup> decay curves with SPP<sup>+</sup>/BP<sup>+</sup> decay curves leads to the conclusion that both <sup>1</sup>RPs and <sup>3</sup>RPs are produced in the former case, the temporal behavior at early times being dominated by field-insensitive <sup>1</sup>RP and at later times by highly field-sensitive <sup>3</sup>RPs. In the case of the SPP<sup>+</sup>/BP<sup>+</sup> system, on the other hand, <sup>3</sup>RPs dominate the decay throughout but the field sensitivity is reduced. The large MFE in O-analogues is presumably caused by reduction of micellar escape rate while the reduced MFE for the S-analogues has been ascribed to spin-orbit coupling (SOC).

## Introduction

In recent years photoinduced electron transfer (PIET) reactions, both forward and backward, have received considerable attention as potential light-harnessing systems.<sup>1–3</sup> The dynamics of the back electron transfer process (BET) is no less interesting than that of the forward electron transfer process (FET) for the following reasons: In any PIET-based energy storage model the extent of energy storage depends critically on the slowness of BET, the latter tending to nullify the chain processes initiated by FET. Second, one can observe beautifully the blending of spin-evolution with spatial motion of radicals generated by FET. One of the interesting consequences of this blending is that a laboratory magnetic field, despite the smallness of its interaction with the radical pair (RP) system, can alter substantially the lifetimes of RPs, thereby providing us a handle for controlling the energy storage process by the turn of a knob. This magnetic field effect (MFE) on the spin dynamics can be magnified by confining in the micelle an electron donor/acceptor system, or more correctly, a RP system.<sup>4–7</sup> A micelle provides a cavity for the photogenerated RP in which the partners of a RP undergo multiple collisions and between two successive collisions the relative spin orientation of the partners changes.<sup>8–10</sup> For understandable reasons, MFE studies so far involve mostly light atom centered (C, N, O) radicals.<sup>9</sup> Recently investigations<sup>11–18</sup> have extended MFE studies to S-, Si-, and Ge-centered radicals. In heavy atom centered radicals isotropic *g*-values deviate from the free electron<sup>14,19</sup> value due to spin-orbit coupling (SOC), and hence, relative precession rates around the applied field (determined by isotropic  $\Delta g$ ) become faster; thus MFE attributable to the  $\Delta g$  mechanism ( $\Delta g$ -M) increases with field. However, other mechanisms, such as the Relaxation Mechanism (RM)<sup>20</sup> and the Triplet Mechanism (TM), may also have

prominent roles to play in recombination dynamics. In heavy atom substituted RPs especially, the field-independent SOC-induced ISC process mixes singlet and triplet states and thereby allows recombination even in the triplet state. These reasons make a case for investigation of other RPs containing heavy atoms, such as (S, Se, Ge), and compare the results with corresponding light atom (C, N, O) centered RPs.

Recently, we have investigated extensively MFEs on transient RPs generated by PIET from a neutral donor, biphenyl, to various derivatives of the phenyl pyrilium salt (positively charged acceptors) in SDS micellar medium.<sup>5–7,21</sup> The observed MFEs in these RP systems are exceptionally large and vary interestingly among derivatives. In our quest for understanding the source of large MFEs in these systems, we have extended our investigation to RPs generated from corresponding thio-pyrilium salts. The present paper is essentially a comparative MFE study of RPs generated from phenyl thio-pyrilium (SPP<sup>+</sup>CIO<sub>4</sub><sup>-</sup>) salt with those generated from the corresponding O-centered phenyl pyrilium salt (PP<sup>+</sup>CIO<sub>4</sub><sup>-</sup>) in SDS micellar solution; the donor is neutral biphenyl in both cases.

## Experimental Section

2,6-Dimethylphenyl pyrilium (PP<sup>+</sup>) perchlorates and the corresponding thio derivatives were prepared by one of us<sup>22</sup> and used after recrystallization twice from dichloromethane and anhydrous ether. The SDS was purified by recrystallization from a water-ethanol mixture. Biphenyl (Aldrich) was used without any further purification. Triply distilled deionized water was used for the preparation of solutions. All the solutions were deaerated by purging Argon for 30 min. The concentrations employed in the experiment were [PP<sup>+</sup>] =  $\sim 1 \times 10^{-4}$  (M), [BP] =  $\sim 1 \times 10^{-3}$  (M), and [SDS] = 0.1 (M).

The experiments were carried out in conventional laser flash photolysis (LFP) setup (laser kinetic spectrometer, Applied Photophysics), coupled and synchronized with a small pulsed electromagnet. The basic circuitry of this setup is described

\* Corresponding author. Fax: +91-33-473-2805. E-mail: pcmc@mahendra.iacs.res.in.

<sup>†</sup> Indian Association for the Cultivation of Science.

<sup>‡</sup> Regional Research Laboratory.

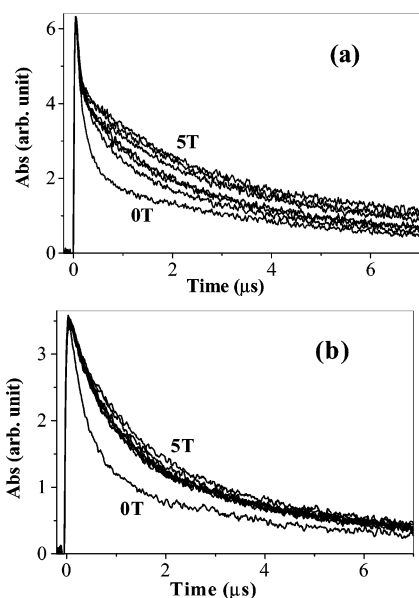
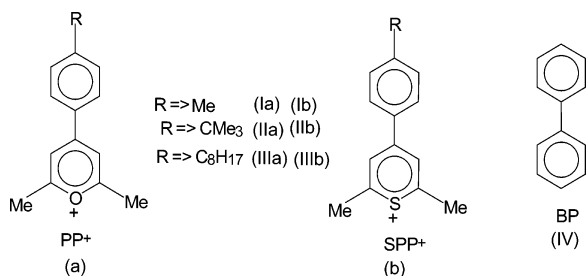


**Figure 1.** Decay profile of the transient absorption at 680 nm for acceptor/donor pair (a) **Ia**/BP and (b) **Ib**/BP in the presence of various external high fields.

elsewhere.<sup>23</sup> The pulse current is provided by the discharge of two parallelly connected capacitors (500  $\mu$ F, 4 kV each) through a mercury ignitron, the latter being triggered by the discharge of another capacitor bank with the help of a thyristor and a pulser unit. The pulse duration for the main capacitor discharge bank is about 2 ms. We have ensured that in the time scale of our experiment, magnetic field remains constant at the maximum in the discharge curve. The magnetic field was calibrated by the surge-coil technique. For our LFP studies we have used the third harmonic (355 nm) of a Nd:YAG (DCR-11, Spectra Physics) laser as the pump source, and a 250-W pulsed xenon lamp as the monitoring source. The output signal from a photodiode was processed by means of a personal computer. The transient signal at each wavelength was averaged over 10 shots. The possibility of change in the solution itself brought about by the flash and/or pulsed field was carefully checked in the following way. The decay curves were obtained for zero-field first and then for the highest field with the same freshly prepared degassed solution. The order of the highest and the zero-field experiment was then reversed with the same sample. Results on two fresh solutions, identically prepared and degassed, compared very well.



## Results and Discussion

In the present study, we have chosen BP as donor and three sets of alkyl derivatives of phenyl pyrlium salt (PP<sup>+</sup>) and the corresponding thio-analogues (SPP<sup>+</sup>) as acceptors. The dynamics of correlated RPs in the presence of fields of various magnitudes are shown in Figures 1a,b, 2a,b, and 3a,b. The salient features of the decay curves are summarized below.

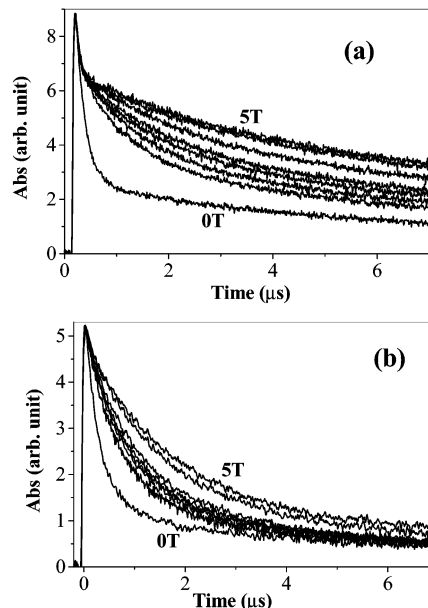


**Figure 2.** Decay profile of the transient absorption at 680 nm for acceptor/donor pair (a) **IIa**/BP and (b) **IIb**/BP in the presence of various external high fields.

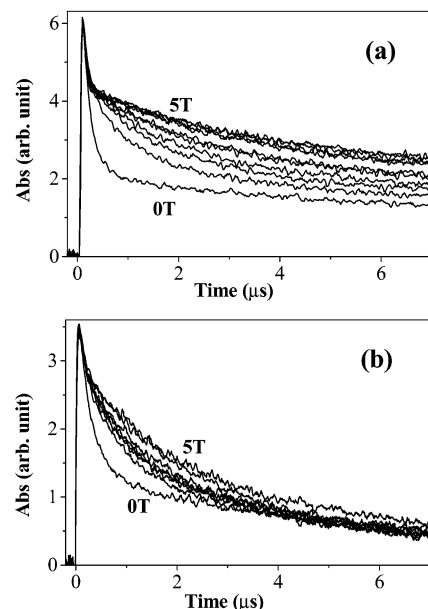
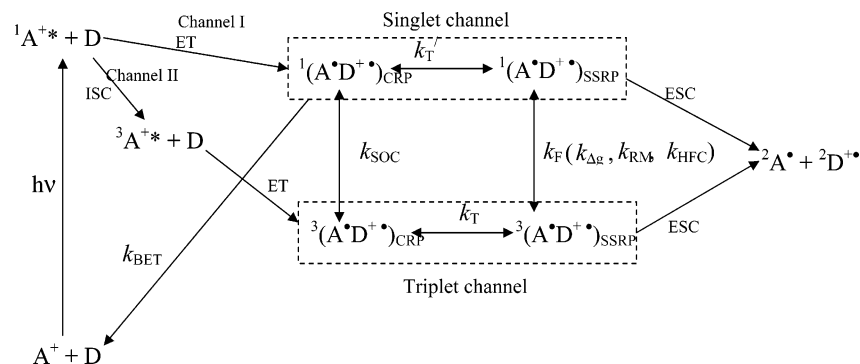


**Figure 3.** Decay profile of the transient absorption at 680 nm for acceptor/donor pair (a) **IIIa**/BP and (b) **IIIb**/BP in the presence of various external high fields.

**Assignment of the Reaction Intermediates.** Different alkyl group substituted PP<sup>+</sup> derivatives and their thio analogues on excitation behave as typical electron acceptors, the donor being unexcited BP or other similar aromatic hydrocarbons. The electron transfer of these systems has been studied by Monoj et al.<sup>22,24</sup> The photochemical behavior of the PIET in SDS micellar solution are qualitatively similar in nature to that in homogeneous medium. It is reasonable to assume that the uncharged donor is trapped in the micellar core, while the positively charged acceptor is drawn out of the bulk water medium to the negatively charged micellar–water interface. Since no MFE is observed in the absence of micelle, we conclude that the water-soluble PP<sup>+</sup> or SPP<sup>+</sup> must have accumulated in the Stern layer of the micelle. The transient

## SCHEME 1



absorption spectra of the RPs observed immediately after laser excitation of the acceptor ( $PP^+$  or  $SPP^+$ ) have been shown elsewhere.<sup>7</sup> The peak around 385 nm is due to  $PP^+$  radicals and that around 680 nm is due to the  $BP^{+•}$  radical. Similar transient absorption spectra are observed for the S-substituted  $PP^+$  ( $SPP^+$ ) acceptors also, where the position of the absorption peak of the  $SPP^+$  radical is shifted to 430 nm from 385 nm.

It is found by Monoj et al.<sup>22</sup> that in homogeneous medium the radical  $BP^{+•}$  is the only one that absorbs at 680 nm. We have also found the same in micellar medium. At 385 nm in the case of  $PP^+$  radicals and at 430 nm in case of  $SPP^+$  radicals, both the molecular triplet and the radical absorb. Consequently, the analysis of the dynamics of RPs at these wavelength windows (385 nm for  $PP^+$  and 430 nm for  $SPP^+$ ) gets complicated. We therefore consider first the features of the time profile of transient absorption ( $A(t)$ ) curves at the 680-nm window before considering the more complicated  $A(t)$  curves at the 385- or 430-nm window. We may point out here that for measuring the recombination rate, it should not matter which radical is monitored. If any one of the partners of a RP leaves the micellar cage recombination is not possible. Thus the overall recombination rates should be expected to remain independent of the choice of wavelength window.

Tanimoto et al.<sup>4</sup> have shown that in bimolecular micellar reactions at high quencher and micellar concentrations intermicellar processes could occur in addition to intramicellar ones. However, at the concentrations studied by us, we have not found evidence for significant intermicellar processes.

**MFEs on Escape Free Radical Yields and Lifetimes.** We draw attention to the following features of decay curves:

(1) Immediately after excitation there occurs a fast decay before the comparatively slow decay takes over. The fast decay part in the time range  $<0.2 \mu\text{s}$  is much more prominent in the  $PP^+/BP$  system than in the corresponding  $SPP^+/BP$  system for all three pairs of acceptors. This fast decay part is insensitive to the magnetic field and essentially corresponds to the behavior of singlet  $^1RP$ .<sup>7</sup>

(2) For times greater than  $3 \mu\text{s}$ , the change of  $A(t)$  with time is negligible. The curves obtained for different fields are all parallel to each other. The value of  $A(t)$  when time is equal to  $6 \mu\text{s}$  has been arbitrarily chosen as a measure of the escape radical yield; it is much less for the  $SPP^+/BP$  system in comparison to the corresponding  $PP^+/BP$  system, in the absence of a magnetic field. The magnetic field induced change is small for the S-analogue in comparison to that for the O-analogue.

(3) For times between 0.2 and  $3 \mu\text{s}$  the values of  $A(t)$  are very sensitive to both time and field. This part of the decay curves corresponds to  $^3RP$  decay and the MFE can as well be estimated from the lifetime measurement at different fields.

(4) On adding the  $Gd^{3+}$  ion (10 mM) to either the  $PP^+/BP^{+•}$  or the  $SPP^+/BP^{+•}$  system, the MFE is nearly completely quenched.

We discuss qualitatively the dynamic behavior of the RP systems,  $PP^+/BP^{+•}$  and  $SPP^+/BP^{+•}$ , with reference to Scheme 1.<sup>25</sup>

At first the positively charged pyrylium or thio-pyrylium ion is excited to the singlet state. Then, in the presence of BP an electron transfer (ET) takes place from neutral donor BP to the singlet acceptor  $^1PP^+$  or  $^1SPP^+$  to form  $^1RP$  of contact and/or solvent-shared type. This singlet channel faces competition from the triplet channel, which is initiated by intersystem crossing (ISC) from the excited singlet acceptor. The  $^3A$  then generates  $^3RP$  by electron transfer from the BP. Dissociation of the  $^1,^3CRP$  to  $^1,^3SSRP$  should be considered as a reversible process, which means that the geminate  $^3SSRP$  can recombine via  $^1CRP$  formation. The singlet and triplet RPs thus produced get converted to triplet and singlet RP respectively by several possible mechanisms, such as SOCM,<sup>25,26</sup>  $\Delta g$ -M,<sup>14,19,27</sup> RM,<sup>20</sup> HFCM,<sup>15,16,18</sup> and TM.<sup>28</sup> Out of these, the first one (SOCM) is independent of applied laboratory field. It may be noted that in a contact radical pair involving light atom centered (O) radicals, no significant  $S \leftrightarrow T$  conversion is expected to occur when the exchange interaction is too large as for a small separation distance between radical partners. However,  $S \leftrightarrow T$  conversion is possible through SOC interaction for a CRP involving heavy atom centered (S) radicals.<sup>9</sup> Note that although SOC is not effective in bringing about the ISC process in  $SSRP$ , it can do so in  $CRP$ ; this point has been dealt with in detail by Steiner et al.<sup>29</sup> Finally, free radicals with long lifetimes are produced by the escape of any one of the partners from the micellar cage. There follows then a competition between escape and recombination (via  $^1CRP$ ).

Although the intermediates in both channels are similar, the time constants for creation or annihilation of intermediates are different, and this determines the shapes of the decay curves significantly. The BET rate in singlet RP being very fast, the  $^1RP$  dominates the decay behavior in the initial time domain ( $<0.2 \mu\text{s}$ ). The SOC-induced ISC rate in the O-centered  $PP^+$  radical is expected to be less than that of the S-centered  $SPP^+$  radical. The singlet channel therefore may dominate in the case of  $PP^+$ , as observed. However, the singlet and triplet yields of  $PP^+$  and  $SPP^+$  in the absence of the donor have been measured directly by Monoj et al.;<sup>22</sup> curiously, the ratios  $\phi_T/\phi_S$  have been found to be nearly the same for  $PP^+$  and  $SPP^+$ . The reason for this difference in behavior between cation and corresponding radical could be the following. The SOC, which induces ISC in the cations, is a function of the atomic number of the heavy nucleus and also the charge density at the heavy atoms. Though the S atom has a higher atomic number than the O atom, the

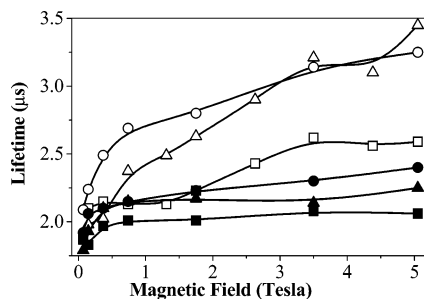


**Figure 4.** Plot of the radical lifetime as a function of magnetic field: □, ○, and △ for the RP generated from compounds **Ia**, **IIa**, and **IIIa**, respectively, and ■, ●, and ▲ for respective thio compounds at 680 nm.

charge density on the S atom in the  $SPP^+$  cation is less than that on the O atom in the corresponding cation. Indeed, the directly measured quenching constants by donors measured by Monoj et al.<sup>22</sup> were found to be greater for  $SPP^+$  compared to  $PP^+$ . In the presence of BP the measured yield of  $^3RP$  is much larger in  $SPP^+$  compared to  $PP^+$ . This explains why the initial decay curves are dominated by the  $^1RP$  channel for the O-centered  $PP^*$  radical, but not so for the S analogue (Figure 6). The field sensitivity of the singlet channel is expected to be small, as is indeed observed for the fast decay component.

In the time domain greater than  $0.2 \mu s$  the decays are dominated by  $^3RPs$  which have long lifetimes, and the relevant route is the triplet one.  $^3RPs$  get converted to  $^1RPs$  where the fast spin-conserving BET process causes the RP to decay. As already pointed out, unlike the  $PP^+/SPP^+$  cations the SOC parameter for the corresponding radicals could be considerably higher due to higher electron density on the heteroatom. The larger SOC in  $SPP^*$  can significantly influence the dynamical route followed by  $^3CRP$ , which gets converted to either  $^3SSRP$  or  $^1CRP$  (Scheme 1). Assuming  $k_{BET} \gg k_{SOC}$ , the yield of  $^3SSRP$  is determined by the factor  $k_T/(k_{SOC} + k_T)$ , where  $k_{SOC}$  gives the rate of conversion to  $^1CRP$  and  $k_T$  represents the rate of conversion to  $^3SSRP$ .

At the  $^3SSRP$  stage again, a  $^3SSRP$  has the option to follow two alternative routes: (1) one of the partners of RP may escape from the micellar cage leading to free radicals of very long lifetime, or (2) there may be spin evolution leading to  $^1SSRP$  and eventual decay of the RP. There could be three field-dependent mechanisms by which  $^3SSRP$  can be converted to  $^1SSRP$ , namely, HFCM,  $\Delta g$ -M, and RM. Out of the three HFCs, interaction arises from the H atom in the BP radical, which is common between the two RP systems. The two radicals  $SSP^*$  and  $PP^*$  have similar structures. Both S and O atoms (as also the C atom) have no magnetic nuclei. Only H atoms have magnetic nuclei, but their number and nature remain very much the same. The observed field variations of escape yields and lifetimes for the two types of  $^3RP$  are shown in Figures 4 and 5. The method for the estimation of  $^3RP$  lifetimes and escape radical yields were discussed in our previous publication.<sup>7</sup> Although there is relatively rapid field variation at low fields, the  $B_{1/2}$  values (if they can be defined at all in the present case) are considerably higher than that expected for HFCM.

The second mechanism that can convert a  $^3SSRP$  to  $^1SSRP$  is  $\Delta g$ -M. A difference in isotropic  $g$  tensor between the two partners of a RP may cause a difference in the rates of precession of the partners around the applied field resulting in  $S \leftrightarrow T_0$  spin re-alignment. With an increase of field, the difference in precession rates is increased leading to faster conversion of  $^3SSRP$  to  $^1SSRP$ , thereby causing a decrease in  $^3RP$  lifetime.

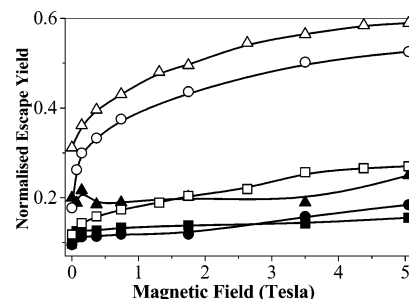


**Figure 5.** Plot of the escape yield of the radical as a function of magnetic field: □, ○, and △ for RPs generated from compound **Ia**, **IIa**, and **IIIa**, respectively, and ■, ●, and ▲ for respective thio compounds at 680 nm.

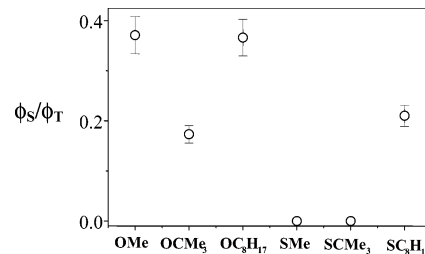
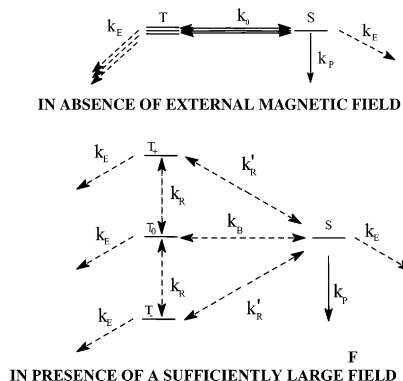


**Figure 6.** Plot of the ratio of singlet and triplet radical pair quantum yields ( $\phi_s/\phi_T$ ) as a function of different alkyl substitution.

## SCHEME 2

### DETAILS OF INTERSYSTEM CROSSING PROCESSES OF SSRP



Hayashi et al.<sup>30</sup> have suggested a method for distinguishing  $\Delta g$ -M and RM. In the presence of  $Gd^{3+}$  (10 mM) a coupling between  $Gd^{3+}$  and  $^3SSRP$  causes a total suppression of MFE due to  $S \leftrightarrow T_{\pm}$  relaxation by RM, but the MFE due to  $\Delta g$ -M remains unaffected by  $Gd^{3+}$  addition. MFE studies were therefore carried out by us in the presence of  $Gd^{3+}$  (10 mM), with the hope that unquenched residual MFE should provide an estimate of the contribution due to  $\Delta g$ -M. When this test was applied to the two types of RPs, we find negligible residual MFE. We, therefore, conclude that the contributions to MFE from both  $\Delta g$ -M and HFCM are negligible for both  $PP^*/BP^{++}$  and  $SPP^*/BP^{++}$  systems; obviously, the MFE in these systems arise from ( $S, T_0 \leftrightarrow T_{\pm}$ ) RM.

We interpret our results on the basis of RM, a model (Scheme 2) proposed by Hayashi et al.<sup>9,20</sup> Scheme 2 is essentially the same as Scheme 1. In Scheme 2 the intrasublevel-dependent kinetics have been highlighted and the multistep back processes via  $^1CRP$  formation have been condensed into a single recombination rate constant  $k_P$ . The cage recombination is assumed to occur from only the singlet  $^1RPs$  with rate constant  $k_P$  (of the order  $10^8$ – $10^9 s^{-1}$ ). The magnitudes of spin relaxation rates

( $k_R$ ,  $k_R'$ ) and the escape rate ( $k_E$ ) in the micelle are similar (of the order  $10^4$ – $10^6$  s $^{-1}$ ). The time profile of concentration (RP( $t$ )) of RP can approximately be represented as follows.

At  $B = 0$ ,

$$\text{RP}(t) = \exp\left[-\left(\frac{k_p}{4} + k_E\right)t\right] \quad (1)$$

At  $B = B_L$ ,

$$\text{RP}(t) = \frac{1}{3} \exp(-k_2 t) + \frac{2}{3} \exp(-k_3 t) \quad (2)$$

Here  $k_2 = k_p/2 + k_3$  and  $k_3 = k_R + k_R' + k_E$ .

Since  $k_p \gg k_R$ ,  $k_R'$ , and  $k_E$ , the lifetime of radical RP (inverse of rate constant) at high fields is governed by the second term of eq 2; hence, the lifetime corresponds to  $1/(k_R + k_R' + k_E)$ .

The transition probability of S,  $T_0 \leftrightarrow T_{\pm}$  due to relaxation mechanism is as follows

$$k_R \propto P\langle T_{\pm}/T_0, S \rangle = \sum \frac{|V_i|^2}{\hbar^2} \frac{2\tau_i}{1 + \omega^2 \tau_i^2} + \sum \frac{|V_{ab}|^2}{\hbar^2} \frac{2\tau_{ab}}{1 + \omega^2 \tau_{ab}^2} \dots \quad (3)$$

$V_i$  ( $i = a$  or  $b$ ) contains the contribution from the anisotropic term of  $g^i$  and  $A^i$  (HFC) tensor and  $V_{ab}$  is due to the dipole–dipole interaction between radicals  $a$  and  $b$ .  $\tau_i$  and  $\tau_{ab}$  denotes the rotational correlation time of the radical and RPs, respectively. On increasing the magnetic field, the precessional motion ( $\omega$ ) of the radical is enhanced, which causes a decrease in relaxation rates ( $k_R$ ,  $k_R'$ ).

We can introduce two limiting situations for  ${}^3\text{RP}$  decay in the presence of a magnetic field

$$\text{Case I: } k_R, k_R' \leq k_E$$

The lifetime  ${}^3\text{RP}$   $1/(k_R + k_R' + k_E)$  in the presence of magnetic field is also dependent on the field-independent escape rate ( $k_E$ ). In this case, the magnetic field induced changes could be low and depend on the relative magnitude of  $k_R$  and  $k_E$ .

$$\text{Case II: } k_R, k_R' \gg k_E \approx 0$$

In this case the lifetime of  ${}^3\text{RP}$  corresponds to  $1/(k_R + k_R')$ , i.e., for negligible escape rate, the lifetimes of the RPs depend only on magnetic field sensitive relaxation rates; magnetic field induced change could, therefore, be large.

A number of transient absorption studies have reported MFEs on triplets $^{31-33}$  of neutral or ionic biradicals where the magnitudes of MFEs were found to be large in comparison to corresponding unlinked RP systems. $^{34}$  Similar large MFEs have also been observed in exciplex emissions of singlet biradicals. $^{35}$  A bridge between the radical centers can indeed reduce the rate of escape of radicals drastically. Tanimoto et al., for example, $^{31}$  has observed a steep increase of RP lifetime generated from linked xanthene–xanthone species on application of a magnetic field. In our previous papers, $^{6,7,21}$  we ourselves have reported some cases of large MFEs in unlinked systems. The point to note about the present system is its interesting spatial distribution within and at the periphery of the SDS micelle. BP should localize within the micellar core while  $\text{PP}^+$  should prefer to localize at the micellar periphery. After electron transfer, the positively charged  $\text{BP}^{*+}$  radical seeks the surface of the micelle, while the neutral  $\text{PP}^*$  radicals move to the micellar core. The

inward motion of the uncharged  $\text{PP}^*$  radical and the outward motion of the  $\text{BP}^{*+}$  cationic radical effectively confine these RPs within the micelle and thereby reduce the escape rate. The situation, therefore, is somewhat similar to that of a linked system. We tentatively conclude that the reduction of the escape rate from the micelle is the cause of large MFE in this case.

Previously, Nishizawa et al. observed that MFE in the case of photoreduction of benzophenone in SDS micellar medium $^{36}$  showed saturation at a field strength of 3 T. They suggested that the saturation originated from the fact that  $k_E$  of their system was larger than  $k_R + k_R'$ . Thus, when  $k_E > k_R + k_R'$ , the  ${}^3\text{RP}$  lifetimes at high fields are mainly determined by the field-independent  $k_E$  value, even though the relaxation rate changes with increasing magnetic field. In the present case, we assume the escape rate to be negligibly small compared to the relaxation rate. As a result, the  ${}^3\text{RP}$  lifetime depends on the field dependent rate constants ( $k_R$ ,  $k_R'$ ). We find that the  ${}^3\text{RP}$  lifetime or the escape radical yield continues to increase with field without saturation for both types of  ${}^3\text{RP}$  ( $\text{PP}^*/\text{BP}^{*+}$  and  $\text{SPP}^*/\text{BP}^{*+}$ ).

The yield of the escape radical observed in the  $\text{SPP}^*/\text{BP}^{*+}$  RPs at zero field is smaller than that in  $\text{PP}^*/\text{BP}^{*+}$  RPs at zero field. The MFEs on the escape radical yield observed in the  $\text{SPP}^*/\text{BP}^{*+}$  RPs are also smaller than that in the  $\text{PP}^*/\text{BP}^{*+}$  RPs. These two facts can be explained by the enhancement of ISC in CRP by SOCM. According to Scheme 1 outlined above, the escape radical yield should be proportional to two factors:  $[k_T/(k_{\text{SOC}} + k_T)]/[k_{\text{ESC}}/(k_{\text{ESC}} + k_F)]$ , where  $k_T$  and  $k_{\text{ESC}}$  refer to spatial evolution and  $k_{\text{SOC}}$  and  $k_F$  ( $= k_{\Delta g} + k_{\text{RM}} + k_{\text{HFC}}$ ) refer to field-independent and field-dependent parts of the spin evolution process, respectively. The first factor  $[k_T/(k_{\text{SOC}} + k_T)]$ , which can be approximated to ca.  $k_T/k_{\text{SOC}}$  for  $k_{\text{SOC}} \gg k_T$ , should make yields and MFEs smaller for  $\text{SPP}^*$ -RPs compared to  $\text{PP}^*$ -RPs. However, it seems that  $k_{\text{SOC}}$  is not the only term that is different between the two RPs, the  $k_F$  ( $\approx k_{\text{RM}}$  at high fields) could also be different. This may be seen from lifetime analysis. The lifetime observed in the  $\text{SPP}^*$ -RPs at zero field is similar to that in the  $\text{PP}^*$ -RPs at zero field. The MFEs on the lifetime of the triplet RPs in the  $\text{SPP}^*$ -RPs is smaller than that in the  $\text{PP}^*$ -RPs. The lifetime at zero field is given by  $k_p/4 + k_E$ . The value for  $\text{SPP}^*$ -RPs may be similar to that for  $\text{PP}^*$ -RPs. The lifetime in the presence of magnetic field is given by  $k_3$  ( $\approx k_R + k_R'$ ). The  $k_3$  value for S-containing RPs is larger than that for the corresponding O-analogue on account of the relaxation due to the S atom.

To observe the effect of substituents on MFE, we attached different alkyl groups to the acceptors,  $\text{PP}^+$  and  $\text{SPP}^+$ . Although we could not find any regularity in differences in MFEs within either series of RPs ( $\text{PP}^*/\text{BP}^{*+}$  or  $\text{SPP}^*/\text{BP}^{*+}$ ), one interesting generalization could be recognized. The zero-field escape radical yield is enhanced on increasing hydrophobicity of the substituent in the acceptor molecule. The observation holds good for both types of acceptors ( $\text{PP}^+$  and  $\text{SPP}^+$ ) (Figure 5). A plausible explanation could be the following. Since the acceptors ( $\text{PP}^+$  and  $\text{SPP}^+$ ) are positively charged, they prefer to reside at the negatively charged micellar periphery. On attachment of the hydrophobic alkyl group, the acceptor molecules move inside the hydrophobic micellar core where the donor BP is localized. Thus, the separation ( $r$ ) between the radical centers at time  $t = 0$  depends on the nature of the substituent. The distance between radical centers at  $t = 0$  decreases on increasing hydrophobicity. The separation between the radicals in a pair is largest in the case of the least hydrophobic Me substituent and smallest in the case of the  $-\text{C}_8\text{H}_{17}$  derivative. From the relation of  $r$ -dependent exchange interaction,  $J(r) = J_0 \exp(-\xi r)$ , it may

be argued that S and T levels are more nearly degenerate for RPs containing less hydrophobic substituents. Consequently, the <sup>3</sup>RP containing a larger alkyl group should have a lower ISC rate to <sup>1</sup>RP, and hence a lower back electron-transfer rate or higher escape radical yield.

### Summary and Concluding Remarks

We have compared MFEs on RPs photogenerated by electron transfer from the ground state of biphenyl to derivatives of phenyl pyrilium salt in SDS micellar solution. On laser excitation both singlet and triplet channels are activated for O-analogues, but only the triplet channels dominate in the case of S-analogues. The dynamics of the initial fast decay part (time range < 0.2 μs) is independent of applied field for the PP<sup>+</sup>/BP system; this is characteristic of singlet RPs. The absence of a fast initial decay part in S-analogues is presumably due to rapid SOC-induced ISC transition to the triplet state from the initially excited singlet SPP<sup>+</sup>. The reduction in MFE in SPP<sup>+</sup>/BP<sup>+</sup> RP in comparison to PP<sup>+</sup>/BP<sup>+</sup> RP has been ascribed by us to large field-independent SOC interaction in S-containing RPs. In MFEs of both O- and S-containing RPs, the roles played by HFCM and Δg-M are relatively minor; the RM plays a major role. A drastic reduction in escape rate arising from the spatial distribution of radicals within the micelle seems to be responsible for the observed large MFE in this differentially solubilized unlinked charged donor–acceptor system.

**Acknowledgment.** M.C. gratefully acknowledges support received from INSA (Senior Scientist Scheme).

### References and Notes

- (1) Kavasrnos, G. J.; Turro, N. J. *Chem. Rev.* **1986**, *86*, 401.
- (2) Norris, J. R.; Lin, C. P.; Dudil, D. E. *J. Chem. Soc., Faraday. Trans. I* **1987**, *83*, 13.
- (3) Miranda, M. A.; Garcia, H. *Chem. Rev.* **1994**, *94*, 1063.
- (4) Tanimoto, Y.; Takoyama, M.; Itoh, M.; Kakaguki, R.; Nagakura, S. *Chem. Phys. Lett.* **1986**, *129*, 414.
- (5) Halder, M.; Chowdhury, M. *Chem. Phys. Lett.* **2000**, *319*, 349.
- (6) Parui, P. P.; Halder, M.; Gopidas, K. R.; Nath, D. N.; Chowdhury, M. *Mol. Phys.* **2002**, *100*, 2895.
- (7) Halder, M.; Parui, P. P.; Gopidas, K. R.; Nath, D. N.; Chowdhury, M. *J. Phys. Chem.* **2002**, *106*, 2200.
- (8) Salokhov, K. M.; Molin, Y. N.; Sagdeev, R. Z.; Buchachenko, A. L. *Spin Polarisation and Magnetic Field Effect in Radical Reactions*; Elsevier: Amsterdam, The Netherlands, 1984.
- (9) Nagakura, S.; Hayashi, H.; Azumi, T., Eds. *Dynamics Spin Chemistry*; John Wiley & Sons: New York, 1998.
- (10) Steiner, U. E.; Ulrich, T. *Chem. Rev.* **1989**, *89*, 51.
- (11) Wakasa, M.; Hayashi, H.; Mikami, Y.; Takada, T. *J. Phys. Chem.* **1995**, *99*, 13181.
- (12) Wakasa, M.; Hayashi, H. *J. Phys. Chem.* **1996**, *100*, 15640.
- (13) Wakasa, M.; Nishizawa, K.; Abe, H.; Kido, G.; Hayashi, H. *J. Am. Chem. Soc.* **1998**, *120*, 10565.
- (14) Wakasa, M.; Nishizawa, K.; Abe, H.; Kido, G.; Hayashi, H. *J. Am. Chem. Soc.* **1999**, *121*, 9191.
- (15) Wakasa, M.; Sakaguchi, Y.; Hayashi, H. *J. Am. Chem. Soc.* **1992**, *114*, 8171.
- (16) Wakasa, M.; Sakaguchi, Y.; Nakamura, J.; Hayashi, H. *J. Phys. Chem.* **1992**, *96*, 9651.
- (17) Hayashi, H.; Sakaguchi, Y.; Kamuchi, K.; Schnabel, W. *J. Phys. Chem.* **1987**, *91*, 3936.
- (18) Wakasa, M.; Hayashi, H. *Chem. Phys. Lett.* **1994**, *229*, 122.
- (19) Wakasa, M.; Nakamura, Y.; Sakaguchi, Y.; Hayashi, H. *Chem. Phys. Lett.* **1993**, *215*, 631.
- (20) Hayashi, H.; Nagakura, S. *Bull. Chem. Soc. Jpn.* **1984**, *57*, 322.
- (21) Halder, M.; Parui, P. P.; Gopidas, K. R.; Nath, D. N.; Chowdhury, M. *RIKEN Rev.* **2002**, *44*, 53.
- (22) Monoj, N.; Kumar, A. R.; Gopidas, K. R. *J. Photochem. Photobiol. A* **1997**, *109*, 109.
- (23) Misra, A.; Halder, M.; Chowdhury, M. *Chem. Phys. Lett.* **1999**, *305*, 63.
- (24) Monoj, N.; Gopidas, K. R. *Chem. Phys. Lett.* **1997**, *267*, 567.
- (25) Shinya, S.; Katsuki, A.; Akiyama, K.; Tero-Kubeta, S. *J. Am. Chem. Soc.* **1997**, *119*, 1323.
- (26) Katsuki, A.; Akiyama, K.; Ikegami, Y.; Tero-Kubeta, S. *J. Am. Chem. Soc.* **1994**, *116*, 12065.
- (27) Bohne, C.; Alnajjar, M. S.; Griller, D.; Scaiano, J. C. *J. Am. Chem. Soc.* **1991**, *113*, 444.
- (28) Pederson, J. B.; Freed, J. H. *J. Chem. Phys.* **1975**, *62*, 1706.
- (29) Steiner, U. E.; Haas, W. *J. Phys. Chem.* **1991**, *95*, 1880.
- (30) Wakasa, M.; Sakaguchi, Y.; Hayashi, H. *Mol. Phys.* **1994**, *83*, 613.
- (31) Tanimoto, Y.; Takashima, M.; Itoh, M. *Bull. Chem. Soc. Jpn.* **1989**, *62*, 3923.
- (32) Nakagaki, R.; Yamaoka, M.; Takahira, O.; Hirata, K.; Fujiwara, Y.; Tanimoto, Y. *J. Phys. Chem. A* **1997**, *101*, 556.
- (33) Tanimoto, Y.; Samejima, N.; Tamura, T.; Hayashi, M.; Kita, A.; Itoh, M. *Chem. Phys. Lett.* **1992**, *188*, 446.
- (34) Tanimoto, Y.; Takashima, M.; Itoh, M. *Chem. Phys. Lett.* **1983**, *100*, 442.
- (35) Staerk, H.; Kuhnle, W.; Treichel, R.; Weller, A. *Chem. Phys. Lett.* **1985**, *118*, 19.
- (36) Nishizawa, K.; Sahaguchi, Y.; Hayashi, H.; Abe, H.; Kido, G. *Chem. Phys. Lett.* **1997**, *267*, 501.